AIP | Review of Scientific Instruments

Haptic-STM: A human-in-the-loop interface to a scanning tunneling microscope

Luís M. A. Perdigão and Alex Saywell

Citation: Review of Scientific Instruments **82**, 073704 (2011); doi: 10.1063/1.3600572
View online: http://dx.doi.org/10.1063/1.3600572
View Table of Contents: http://scitation.aip.org/content/aip/journal/rsi/82/7?ver=pdfcov
Published by the AIP Publishing

Haptic-STM: A human-in-the-loop interface to a scanning tunneling microscope

Luís M. A. Perdigão[a] and Alex Saywell
School of Physics and Astronomy, University of Nottingham, University Park, Nottingham NG7 2RD, United Kingdom

(Received 14 March 2011; accepted 22 May 2011; published online 19 July 2011)

The operation of a haptic device interfaced with a scanning tunneling microscope (STM) is presented here. The user moves the STM tip in three dimensions by means of a stylus attached to the haptic instrument. The tunneling current measured by the STM is converted to a vertical force, applied to the stylus and felt by the user, with the user being incorporated into the feedback loop that controls the tip-surface distance. A haptic-STM interface of this nature allows the user to feel atomic features on the surface and facilitates the tactile manipulation of the adsorbate/substrate system. The operation of this device is demonstrated via the room temperature STM imaging of C_{60} molecules adsorbed on an Au(111) surface in ultra-high vacuum. © *2011 American Institute of Physics*. [doi:10.1063/1.3600572]

I. INTRODUCTION

Since its invention the scanning tunneling microscope (STM) (Ref. 1) has proven to be a powerful instrument, allowing researchers in a variety of scientific disciplines to study surfaces with atomic resolution. The high resolution images that can be achieved by an STM are due to the close proximity of the probe to the surface and the highly localized nature of the electron tunneling phenomena. By using an appropriate feedback circuit, which measures the electron tunneling while controlling the distance of the probe to the surface, topographic images can be obtained by recording the tip-height and rastering over the surface. This principle of operation has been extended to allow spectroscopic and manipulation studies to be performed. In order to simplify the operation of an STM, tasks such as approaching the tip, topographic imaging, manipulation, and spectroscopy are automated. For example, electronic and digital signal processors perform the tasks of feedback control and simple tip movement, while computer software controls data acquisition. Automation makes the instrument easier to use, reducing the level of user interaction to the choice of scanning parameters and analysis of the images obtained. However, it also distances the user from the instrument and therefore reduces the degree of control the user has over executing fundamental low-level operations.

Rather than relying solely on the visual perception of the user to control the instrument, we can take advantage of the user's tactile perception by allowing the user to experience forces which provide an instantaneous response to changes in the state of the system under study. The forces experienced by the user may be manifested as a macroscopic movement in the three-dimensional (3D) space where the user is situated. A haptic instrument, such as the one described in this article, can provide this functionality by applying a force to a stylus held by the user, in response to the movements that the user applies to the microscope probe. Connecting a haptic device to an STM may improve perception and assist the user with the probing and manipulation of the adsorbate/substrate system being studied. Conceptually, the movement of the haptic stylus is translated to a physical (and scaled) movement of the STM probe in real-time. Depending on the strength of the interaction between the probe and the surface, the haptic device is programmed to respond by applying a force proportional and opposite to the distance between the probe and the surface. This principle of operation is illustrated in Fig. 1.

II. REVIEW

Several examples of a haptic device being coupled to a scanning probe microscope (SPM) can be found in the literature. Tan *et al.*[2] provides a good review of several past efforts, most involving atomic force microscopes (AFM). In haptic devices with more than one degree of freedom, control of the scanning probe on the X-Y plane has been successfully achieved by several groups by simply translating and scaling X-Y coordinates. Implementation of the translation of the Z (tip-surface distance coordinate) motion between the haptic device and the STM, and corresponding vertical forces applied to the haptic device vary between systems. The operational concept of a haptic device connected to an SPM was first shown in a drawing by Hollis *et al.*[3] In the operation of the *magic wrist*, the Z position is compared with the microscope tip position and a vertical force is applied by the haptic device (the *magic wrist*) in order to "force" the user's hand to follow the probe height motion. The *nanoManipulator*[4] allows the user to control the position of the probe when used in free motion mode, the force applied to the stylus is calculated by using the data acquired by the AFM to construct an imaginary hard surface, with the applied force being proportional to the proximity of the haptic tip to this virtual surface. In an older version of the *nanoManipulator*,[5] the force felt by the user is linearly proportional to the difference between the haptic Z position and the actual microscope probe vertical

[a]Author to whom correspondence should be addressed. Electronic mail: luis.perdigao@nottingham.ac.uk. Tel.: +44 115 8568823. Fax: +44 115 951 5180.

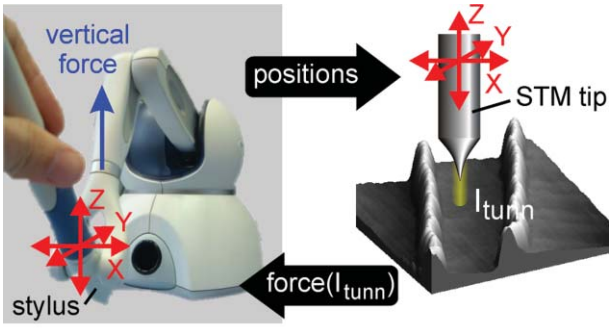

FIG. 1. (Color online) Principle of operation for the haptic-STM interface. User controlled movement of the haptic stylus is translated to STM-tip movements in all axis. The vertical force felt in the haptic device is a function of the tunnel current (I_{tunn}) measured in the STM. The electronic feedback loop is broken and user becomes part of the loop.

position converted to haptic coordinates, identical to the operation of the magic wrist discussed above. Sitti *et al.*[6] used a one degree-of-freedom haptic device, where the Z probe position is controlled using a proportional-integral (PI) controller that tracks the haptic position, and the force-feedback felt in the haptic device is converted from the AFM-probe measured force using a proportional-differential (PD) controller, and adjusted to the applied user force. Teleoperation of an AFM has also been utilised by Iwata *et al.*[7] to perform manipulation and ultrasonic cutting, where the force-feedback applied in the haptic device is adjusted to follow the probe position. During manipulation the force applied by the user is converted to a new setpoint for the atomic force probe. There are also examples where a haptic device is used to provide the user with extra information about surface properties (such as softness and adhesion) which are otherwise difficult to show visually. Technically this is not teleoperation but is augmented reality, since the forces are computed from a created 3D environment based on the microscope measurements.[8,9] A recent attempt to teleoperate an STM in a similar way to that described here was shown by Tan *et al.*;[2] however, they were limited by the speed of bidirectional data communication between the computer and the STM, which prevented efficient incorporation of a human "user" into the feedback loop. Fortunately, this issue has been resolved in the haptic-STM interface presented below. Finally, Jobin *et al.*[10] successfully demonstrated the operation of an AFM in closed-loop operation controlled with a haptic device in performing manipulation of carbon nanotubes and silica beads.

III. THE HAPTIC-STM INTERFACE

The haptic device used in the experiments reported here is a Phantom Omni model (Sensable Technologies). The device is supplied with bundled drivers and an application programming interface (API) for C/C^{++} computing language (called OpenHaptics Toolkit 2.0), with examples provided. Access to the SPM software code (NOTTSPM – originally written in Visual Basic language) is required to include haptic functionality. An ActiveX control was developed that interfaces with the haptic device through methods and properties (Fig. 2). The X, Y, and Z positions of the haptic device are

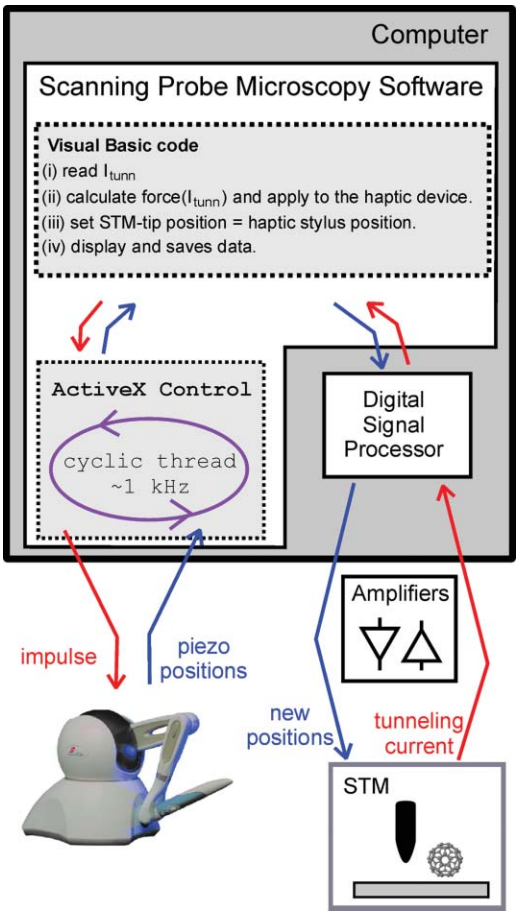

FIG. 2. (Color online) Diagram demonstrating the implementation of the haptic-STM interface. The scanning probe microscopy software is used to interface the STM with the haptic device. Positions of the haptic stylus and forces to be applied are sent to the haptic device through an ActiveX control running a separate software thread. STM positions set by the software and measured tunnel current are passed through the digital signal processor (DSP), running with open feedback loop, and through the amplifiers.

read as object properties, and the forces applied along the three axes are set using an object method. The control can run the high priority thread, called *scheduler*, provided by the API. *Scheduler* uses a callback function within the control that updates position and forces values at ~1 kHz rate, which is essential for smooth operation of the device. The force value sent to the haptic device in each cycle of the thread leads to a small "kick," or impulse, being applied to the servomotor of the haptic device, with the intensity proportional to the supplied force value. It is important that these impulses are passed at a high and constant rate (at least 1 kHz) so that the user feels a smooth continuous force, therefore *haptic force* is a term that corresponds to a physical force only when the cyclic thread (*scheduler*) is used.

It is assumed that the values of the haptic force determined by the SPM software can vary considerably over short periods of time, which could lead to unwanted vibrations when the user operates the device. For this reason, a smoothing routine was implemented within the ActiveX control that simply limits the rate of change of force value applied to the device between each cycle. This routine is optional and can be adjusted before operating the device. An additional

complication was encountered when the haptic device was used to scan over rough surfaces, with rapid changes in Z-force leading to sudden undesired movement in the X or Y axis of the haptic stylus. To reduce this effect an adjustable friction response was implemented where a small force, proportional and in the opposite direction to the change in X and Y positions between cycles, is applied. This friction parameter can be adjusted for each axis individually, although in the experiments discussed here it was only applied to the X-Y plane.

The original SPM software used to control the STM was extended to include a user-friendly graphical user interface (GUI) to facilitate the operation of the haptic device. After working with the STM in conventional mode and acquiring several images the user chooses when to initiate the haptic device by clicking a button which brings up a new window/dialog with options and parameters for the haptic-STM (options are available for interaction type, feedback or touch, and constants of interaction). The last scanned image (unprocessed) is displayed, providing the user with a point of reference for the surface under study. After setting the parameters (or retaining the default values), the user needs to press the "space" key to pass control to the haptic device. The haptic-STM operation only starts when the user presses a button on the stylus which associates the current position of the stylus with the current position of the STM tip. Immediately after haptic-STM operation has commenced the conventional STM feedback routine in the digital signal processor (DSP) (Ref. 11) is disabled and the DSP switches to a transparent mode of operation where it runs a loop that simply passes the tunnel current values from the STM to the SPM software and the X, Y, and Z haptic-positions are passed from the SPM software to the STM at high rate. In the SPM software a cycle starts that follows the following steps: (i) read haptic stylus position; (ii) read tunnel current from DSP/STM, calculate z-force and send to haptic device; (iii) set new STM-tip position based on the haptic stylus position; (iv) display and save data. The operational steps are illustrated in Fig. 2, with arrows indicating the flow of tunneling current information and probe/stylus positions.The user stops the haptic-STM operation by pressing the "space" key or clicking stop button in the GUI. About 417 data points per second are acquired during the haptic-STM operation, without interrupting the haptic control which is running simultaneously in a separate high priority thread in the computer.

The tunnel current (I_{tunn}) measured is translated to a vertical force applied to the haptic stylus in one of two selectable ways. In *touch mode* the haptic force (F_h) is given by

$$F_h = k_{touch} \times I_{tunn}, \tag{1}$$

and in *feedback mode*, the force is calculated using the formula

$$F_h = k_{feeback} \times \log(I_{tunn}/I_{set}), \tag{2}$$

where I_{set} is the setpoint current used during imaging, k_{touch} and $k_{feedback}$ are constants of proportionality that can be set within the program. In *touch mode* the user "feels" a virtual surface where the stylus is subjected to an upward force when the stylus is moved down, the strength of the force is dependent on the magnitude of the measured feedback current. In *feedback mode* the haptic stylus "feels" like it is constrained to an imaginary surface corresponding to the surface topography of a constant current STM image.

The calibration between the movement of the haptic stylus and the STM tip position is performed automatically within the SPM software code. The X-Y coordinates are translated such that the current STM scan dimension (defined in the control panel) is set to a defined haptic range of coordinates. During haptic-STM operation the path of the tip is projected onto a copy of the previously obtained STM image. Regarding the Z-axis, the values for the maximum and minimum height in the last image are associated to a defined Z-axis movement range for the haptic stylus, but this calibration can be changed manually.

IV. EXPERIMENTAL METHODS

The STM experiments were performed under ultra-high vacuum conditions (base pressure $\sim 10^{-11}$ Torr). An Au(111) on mica (Agilent) sample was cleaned by argon sputtering (750 eV, $I_{sample} = 1.4\ \mu$A, $P_{Ar} = 5.2 \times 10^{-6}$ Torr, 40 min) and subsequent annealing at $\sim$400 °C for $\sim$1 h. The cleanliness and characteristic $22 \times \sqrt{3}$ reconstruction (double zigzag pattern) was confirmed with STM.[12] C_{60} was sublimated from a Knudsen cell at 415 °C.

V. RESULTS AND DISCUSSION

The STM images of the Au(111) surface acquired after the submonolayer deposition of C_{60} show that the molecules form small islands which nucleate at step edges, consistent with previous studies.[13,14] A region of the surface containing a step edge decorated with C_{60} was chosen for the operation of the haptic-STM in *feedback mode* (STM images shown in Fig. 3). The faint double lines perpendicular to the step edge are characteristic of the herringbone $22 \times \sqrt{3}$ reconstruction.[12] During haptic operation, the STM tip followed the path of the haptic stylus as controlled by the user. In order to assist the user, the path is displayed in real-time during operation by overlaying the tip trajectory on the last image obtained. The path is drawn in grayscale with white corresponding to higher haptic stylus height (or tip height), in analogy with the color scale of the original image. The path of the tip during haptic operation ($\sim$12 s) is shown in Fig. 3(a), with the trajectory followed illustrated by an arrowed line in Fig. 3(b). It is clear from the trajectory that the user has felt the height increase associated with the C_{60} molecules attached to the step edges. Figure 3(c) shows a plot of the haptic Z position as a function of time while the stylus was moved along the trajectory. The predicted tip-height for the tip following the same path, over the same region of the surface, in constant-current feedback conditions (without the haptic device) is also plotted in Fig. 3(c). There is a good match between the haptic Z and the predicted Z positions, indicating that the user's hand, holding the stylus, followed the surface as if the tip was in current feedback mode. The first peak observed in the haptic trace matches with a step-edge feature, with the slight mismatch attributed to thermal

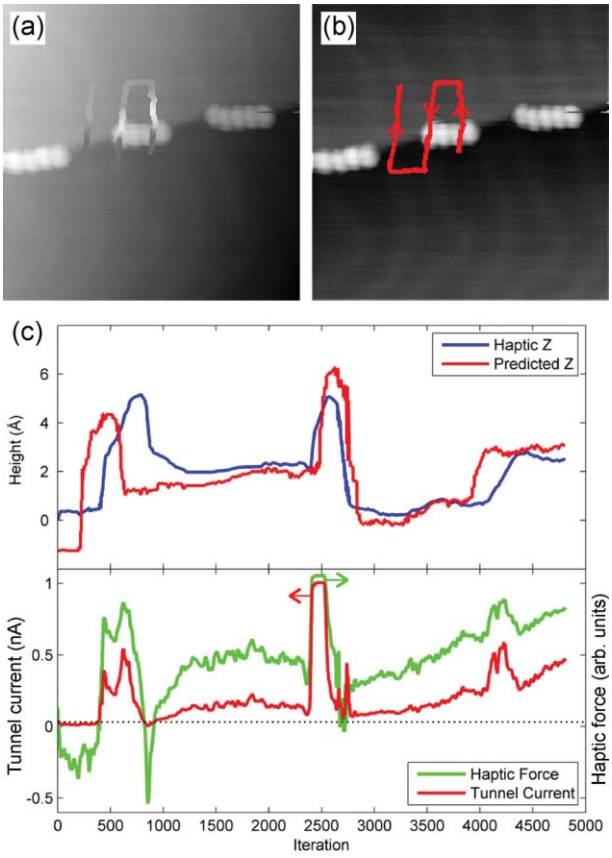

FIG. 3. (Color online) An example of the haptic-STM operating in *feedback mode* using Z conversion 0.271 Å/cm (STM scale / haptic scale) and force response constant set to 0.3. (a) and (b) are STM images of the surface (230×230 Å^2, -1.8 V, 0.03 nA) with the superimposed trajectory of the STM tip controlled by the haptic device. The grayscale trajectory in (a) represents the Z position, with white and dark corresponding to higher and lower tip-surface distances. In (b) the image is plane-corrected and the trajectory is represented with an arrowed line indicating the direction taken. (c) shows plots of the height and force applied data acquired during the haptic-STM operation. In (c), top graph, the Haptic Z line is the height of the STM tip as controlled by the haptic device and the Predicted Z line is the calculated tip height along the same trajectory if the feedback loop was on (constant current mode without haptic operation) as obtained from the last STM image obtained. In (c), bottom graph, are the measured tunnel current and the vertical force applied (see Eq. (2)) to the haptic device during operation, with the arrows pointing to their associated scalebar.

drift. The next peak in the tunnel current trace is a transition from a high terrace to a low terrace (with C_{60} adsorbed at the step edge) and is clearly identical to the path followed by user/haptic stylus. The last feature observed is the transition from a low terrace to a high terrace via a step edge (with no adsorbed C_{60}) where, as expected, the change in height is smaller than for the situation with adsorbed C_{60}. However, the response of the haptic Z appears to be slower than that of the predicted Z response. The lower plot in Fig. 3(c) shows the measured tunneling current (I_{tunn}) and the force applied to the haptic device (calculated from I_{tunn}). Surface features which give rise to an increase in I_{tunn} are generally accompanied by a large upward force applied to the haptic device, which is expected, in order to try to maintain the feedback condition. Descending topographic features result in I_{tunn} momentarily being lower than I_{set} (horizontal line), resulting in a downward haptic force being applied.

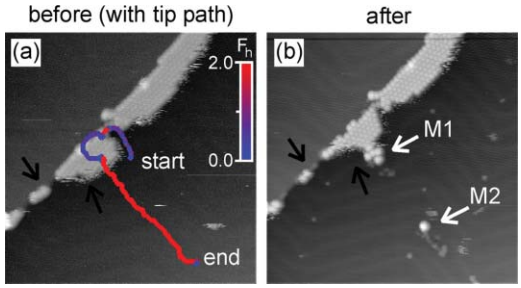

FIG. 4. (Color online) An example of haptic-STM manipulation. (a) is an STM image obtained (500×500 Å, -1.8 V, 0.03 nA) before manipulation with the manipulation trajectory overlaid in color, which represents the tunnel current or haptic force intensity (see scale bar). Also indicated are the initial and final positions of the scanning probe. The black arrows indicate features on the surface which are present before and after manipulation. The image shows a C_{60} close-packed island nucleated on a step edge of Au(111) reconstructed surface. The trajectory passes over the C_{60} island, where the probe is pressed against the surface using the haptic interface, and dragged to a clear Au(111) region. The haptic-STM was set to *touch mode,* with $k_{touch} = 2.0$. (b) is the STM image taken after the haptic manipulation, with the black arrows pointing to the same features as the arrows in (a), and the white arrows labeled as M1 and M2 highlighting changes to the surface, the fragmentation of the C_{60} island and the appearance of a cluster on the previously clean surface.

It is clear from the plots that stability of the human-in-the-loop control is not an issue in this experiment. The correct choice of operational parameters prevents issues relating to tip-surface contact. In particular, the C_{60} height is $\sim$7 Å which is significantly higher than that of the Au steps (step height = 2.35 Å), therefore moving the tip over such features could potentially lead to sudden changes in tunnel current and consequently a rapid change in the applied haptic forces. A user could conceivably have difficultly following these rapid changes, but such a situation can be prevented by making slow stylus movements and by the implementation of smoothing techniques as discussed earlier. Although in some regions $I_{tunn} > I_{set}$, this may reduce the tip-surface distance by 1–4 Å, which is unlikely to cause tip or surface damage.

Figure 4 shows an example of a manipulation experiment performed with the haptic device in *touch mode*. The color scale of the trajectory represents the tunneling current, or force applied by the haptic device. Manipulation occurs when the user presses the haptic stylus towards the surface. This is clearly highlighted by the color on the trajectory plot of the tip. The trajectory shows that the haptic stylus is pressed down over a C_{60} island and dragged to a clean Au(111) region. The STM image taken after the manipulation in Fig. 4(b) shows that a portion of the C_{60} island has been removed. Additional features are present on the surface after the manipulation, as indicated with white arrows M1 and M2, at the edge of the C_{60} island and on the Au surface, near where the manipulation trajectory ended. The image after the manipulation suggests that the STM tip has removed C_{60} molecules from the intended region. Under the conditions used, the fragmentation of the C_{60} island is likely to be caused by tip manipulation, however the appearance of a C_{60} cluster not attached to a step edge (M2) is only possible at room temperature if an "anchor" exists. This C_{60} cluster is located over a elbow point of the zigzag herringbone reconstruction of the Au(111) surface, which is known

to be a preferred adsorption site for metals deposited on this surface.[15–17] The appearance of bright features located at several of these elbow points in Fig. 4(b) also suggests that additional particles have been adsorbed. The small corrugation of these spots suggests that they are unlikely to be isolated C_{60} molecules but it is possible that this is atomic tungsten removed from the tip, during the manipulation process, and has become adsorbed to the Au surface. We therefore propose that the C_{60} cluster highlighted is attached to a tungsten particle situated at an elbow point.

VI. CONCLUSION

We have described a haptic interface for the operating of a scanning tunneling microscope operating in ultra-high vacuum conditions. The results presented here demonstrate the capabilities of the system, allowing manual control of the scanning probe and molecular manipulation with simultaneous sensory feedback, thus providing tactile access to the nanoscale environment. Such a system demonstrates an alternative method for operating a scanning probe microscope, highlighting potential applications relating to the manipulation and assembly of devices. Additionally, the implementation interface presented here offers the possibility of being be integrated in other scientific instruments and with the advantage of improving accessibility.

ACKNOWLEDGMENTS

This work was supported by the U.K. Engineering and Physical Sciences Research Council (EPSRC) under the Grant No. EP/D048761/1. The authors are grateful to Ben Medford for valuable discussions related to the haptic device and to Professor Peter Beton for providing access to the UHV-STM.

[1] G. Binnig, H. Rohrer, C. Gerber, and E. Weibel, Appl. Phys. Lett. **40**, 178 (1982).
[2] H. Z. Tan, R. Reifenberger, G. Chiu, L. Walker, S. Mahadoo, and A. Raman, in *World Haptics Conference: First Joint Eurohaptics Conference and Symposium On Haptic Interfaces For Virutual Environment and Teleoperator Systems*, Pisa, Italy, 2005 (IEEE Computer Soc, Los Alamitos, CA, 2005), pp. 271–276.
[3] R. L. Hollis, S. Salcudean, and D. W. Abraham, in *Micro Electro Mechanical Systems, 1990. Proceedings, An Investigation of Micro Structures, Sensors, Actuators, Machines and Robots*, Napa Valley, CA, 1990 (IEEE, 1990), pp. 115–119.
[4] M. Guthold, M. R. Falvo, W. G. Matthews, S. Paulson, S. Washburn, D. A. Erie, R. Superfine, F. P. Brooks, and R. M. Taylor, IEEE/ASME Trans. Mechatron. **5**, 189 (2000).
[5] R. M. Taylor, W. Robinett, V. L. Chi, J. Frederick, P. Brooks, W. V. Wright, R. S. Williams, and E. J. Snyder, in *Proceedings of the 20th Annual Conference on Computer Graphics and Interactive Techniques* (ACM, Anaheim, CA, 1993), pp. 127–134.
[6] M. Sitti and H. Hashimoto, IEEE/ASME Trans. Mechatron. **8**, 287 (2003).
[7] F. Iwata, K. Ohara, Y. Ishizu, A. Sasaki, H. Aoyama, and T. Ushiki, Jpn. J. Appl. Phys. **47**, 6181 (2008).
[8] W. Vogl, B. K. Ma, and M. Sitti, IEEE Trans. Nanotechnol. **5**, 397 (2006).
[9] G. Li, N. Xi, M. Yu, and W. Fung, IEEE/ASME Trans. Mechatron. **9**, 358 (2004).
[10] M. Jobin, R. Foschia, S. Grange, C. Baur, G. Gremaud, K. Lee, L. Forro, and A. Kulik, Rev. Sci. Instrum. **76**, 053701 (2005).
[11] M. J. Humphry, R. Chettle, P. J. Moriarty, M. D. Upward, and P. H. Beton, Rev. Sci. Instrum. **71**, 1698 (2000).
[12] J. V. Barth, H. Brune, G. Ertl, and R. J. Behm, Phys. Rev. B **42**, 9307 (1990).
[13] E. I. Altman and R. J. Colton, Surf. Sci. **279**, 49 (1992).
[14] C. J. Satterley, L. M. A. Perdigao, A. Saywell, G. Magnano, A. Rienzo, L. C. Mayor, V. R. Dhanak, P. H. Beton, and J. N. O'Shea, Nanotechnology **18**, 455304 (2007).
[15] D. D. Chambliss, R. J. Wilson, and S. Chiang, Phys. Rev. Lett. **66**, 1721 (1991).
[16] A. W. Stephenson, C. J. Baddeley, M. S. Tikhov, and R. M. Lambert, Surf. Sci. **398**, 172 (1998).
[17] E. I. Altman and R. J. Colton, Surf. Sci. **304**, L400 (1994).